T2066

Development of a Physiologically Based Pharmacokinetic (PBPK) Model for Simulating the Disposition of Antibody Drug Conjugates

Haiying Zhou, Michael B. Bolger, Viera Lukacova

Simulations Plus, Inc., 42505 10th Street West, Lancaster, CA 93534, USA

PURPOSE

Antibody-drug conjugates (ADCs) are a novel class of therapeutic agents that deliver potent cytotoxic drug molecules (payload) to their targets while reducing systemic exposure. ADCs may be composed of heterogeneous mixtures of conjugates with variations in both drug-to-antibody ratio (DAR) and conjugation sites, or homogenous compositions with a controlled DAR and specific sites of conjugation. To understand the complex disposition mechanisms of ADCs, a comprehensive PBPK model was developed in GastroPlus™ (Simulations Plus, Inc.) to simulate the disposition of unconjugated antibody and payload, as well as conjugates with different DARs after ADC administration.

METHODS

The previously developed whole-body PBPK model for unconjugated monoclonal antibodies (mAbs) in GastroPlus was expanded to include mechanisms related to ADC's deconjugation and the production of payload. Similar to unconjugated mAbs, the mechanisms related to the absorption and disposition of ADCs include convective transport, lymph flow, fluid phase endocytosis, pH-dependent FcRn binding, FcRn recycling, endogenous IgG, and target-mediated drug disposition. The cytotoxic payload attached to the antibody can be released and distributed in the body when ADC clearance occurs, both through nonspecific and target-specific mechanisms. Also, higher DAR conjugates may be converted to lower DAR conjugates via the deconjugation of the payload molecule from the antibody in vascular and interstitial spaces (Figure 1). All of these mechanisms are incorporated in each tissue compartment (Figure 2) of the whole-body PBPK model. The released payload is cleared through metabolism or renal excretion.

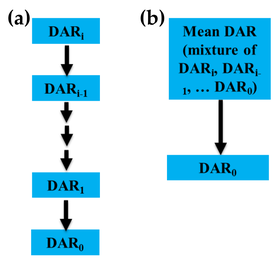

Figure 1: Schematic of ADC deconjugation. **(a)** A series of transit compartments to describe the deconjugation process from higher to lower DARs. Every conjugated payload is assumed to have the same deconjugation rate constant. **(b)** The average DAR is used to describe the deconjugation of ADCs to unconjugated antibody.

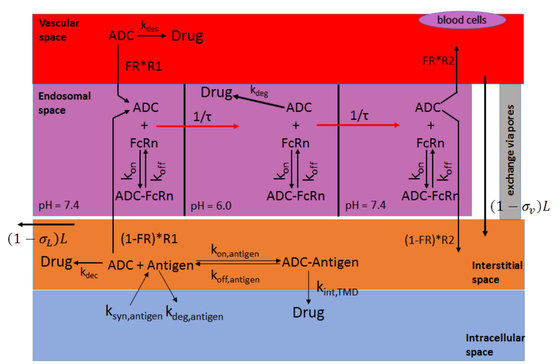

Figure 2: Schematic representation of individual tissue compartments

RESULTS

The PBPK model for ADCs was applied to simulate the pharmacokinetics of Trastuzumab Emtansine (T-DM1) in rat and cynomolgus monkey and an anti-5T4 ADC A1mcMMAF in mice after intravenous administration. The simulated profiles of total antibody, released payload, and conjugates with different DARs were in close agreement with published data for both ADCs (1,2). The same disposition parameters as previously validated for mAb dispositon in mice, rats, and monkeys were used to model the disposition of different DAR conjugates in each species.

For T-DM1, the deconjugation rate constant (0.05 1/d) was fitted to the rat data after administration of the dose with average DAR = 1.5. The same deconjugation rate constant was then used to simulate theT-DM1 dose with average DAR = 3.1 in rat and monkey. The association coefficient between T-DM1 and monkey FcRn at pH=6.0 was estimated using the experimental data.

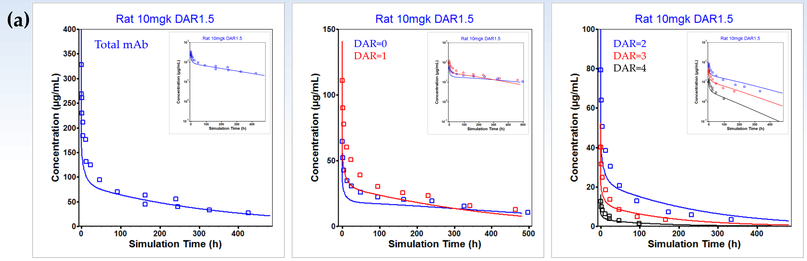

Figure 3: Comparison of simulated (lines) and measured (points) plasma concentrations of total antibody and various DAR conjugates for 10 mg/kg T-DM1 dose with different initial DAR distributions in rats **(a)** average DAR=1.5 (dose contains 1% DAR_5, 4% DAR_4, 13% DAR_3, 26% DAR_2, 35%DAR_1, and 21% DAR_0); and **(b)** average DAR=3.1 (dose contains 2% DAR_7, 5% DAR_6, 10% DAR_5, 19% DAR_4, 26% DAR_3, 23% DAR_2, 13% DAR_1, and 2% DAR_0).

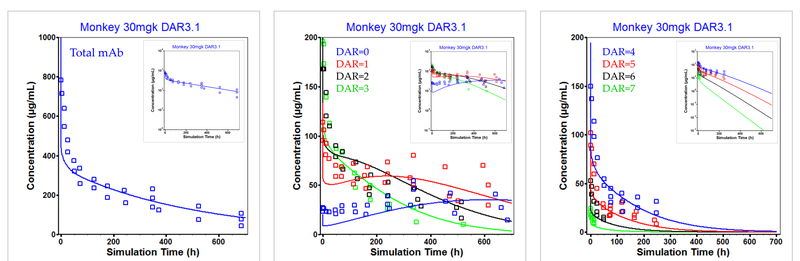

Figure 4: Comparison of simulated (lines) and measured (points) plasma concentrations of total antibody and various DAR conjugates for 30 mg/kg T-DM1 dose with average DAR = 3.1 in cynomolgus monkey The initial distribution of DARs was the same as for the dose with average DAR=3.1 in rat (Figure 3).

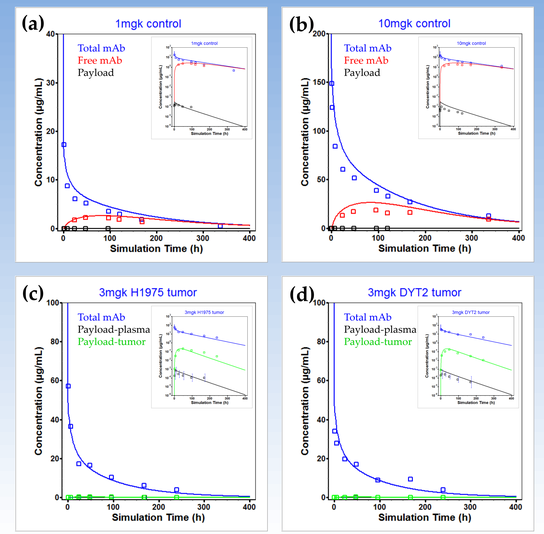

Figure 5: Comparison of simulated (lines) and measured (points) concentration-time profiles of mAb and payload after administration of A1mcMMAF with the average DAR = 4. Individual plots show plasma concentrations of total mAb, free mAb, and released payload in non-tumor-bearing mice after **(a)** 1mg/kg dose, and **(b)** 10 mg/kg dose; plasma concentrations of total mAb and plasma and tumor concentrations of released payload after 3mg/kg dose in **(c)** H1975 tumor bearing mice, and **(d)** DYT2 tumor bearing mice.

The distribution of different DAR conjugates was not available for A1mcMMAF and the average DAR was used to describe the deconjugation for this ADC. The association coefficient between A1mcMMAF and mouse FcRn at pH=6.0 and the ADC deconjugation rate constant were fitted to the reported plasma concentration profiles of total mAb and free mAb after administration of 1mg/kg dose in control mice (no tumor). The same values of these parameters were then used to simulate the free and total mAb concentration profiles after 10mg/kg dose in control mice and 3mg/kg dose in both types of tumor bearing mice. The binding affinity coefficients between mAb and 5T4 (antigen) and the expression levels of 5T4 in H1975 and DYT2 tumor cells were obtained from literature (2).

For the released payload, the specific permeability-surface area product (PStc per mL of tissue cell volume) was used to calculate PStcs for individual tissues. The specific PStc and liver intrinsic clearance were fitted to the reported plasma concentration profile of released payload after administration of a 1mg/kg dose in control mice. To account for the binding effect between released payload and tubulin in tumor cells, the PStc for tumor was estimated using the tumor Cys-mc-MMAF concentration from a 3mg/kg dose in H1975 tumor-bearing mice.

CONCLUSIONS

- PBPK modeling of ADCs incorporating deconjugation models using either detailed DAR distribution or average DAR accurately simulated PK profiles of ADC conjugates
- Using PStc for the released payload distribution, the model predicted released payload concentrations in plasma and tumor reasonably well
- This model could also be applied to assess the important mechanisms that are responsible for released payload concentrations in plasma and tumor compartments

REFERENCES

1. Bender et al., AAPS J, 16 (2014), 994-1008;
2. Shah et al., AAPS J, 16 (2014), 452-463

SimulationsPlus
SCIENCE + SOFTWARE = SUCCESS